Supporting Information

Hydrolysis of Ester Phosphates Mediated by a Copper Complex

Brandon Meza–González and Fernando Cortés–Guzmán *

Facultad de Química, Universidad Nacional Autónoma de México, Ciudad de México, 04510, Mexico

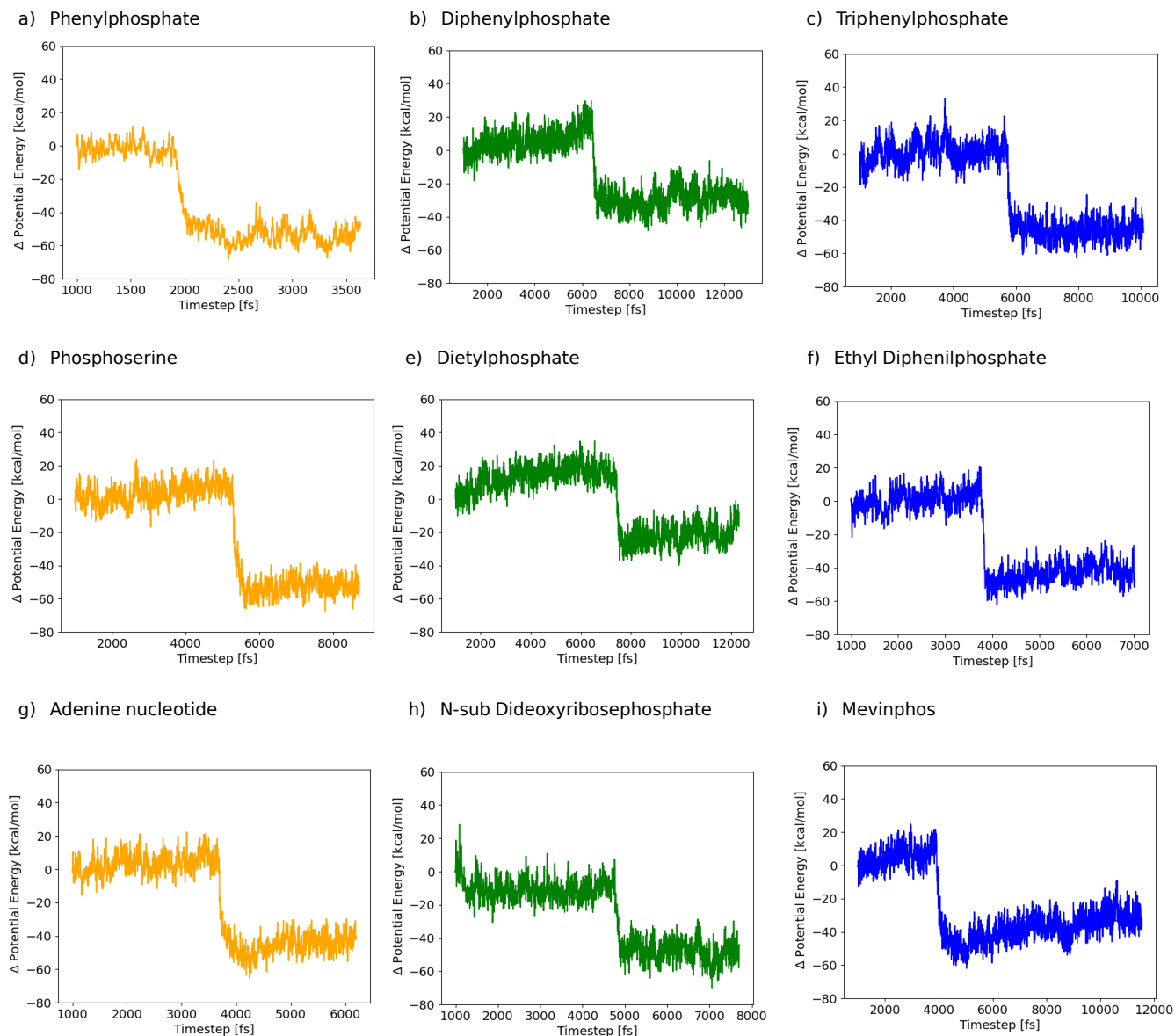E-mail: fercor@unam.mx

Supplementary Figure 1

Figure 1: Calculated potential energy profiles[1] of the set of molecules analyzed in this work. Blue graphs: mono-esters, green: di-esters, red: tri-esters. All energy decreases ($\sim$|50 kcal/mol|) are related to the exit of the leaving group in the hydrolysis process. That is, all reactions occur with a stabilization of the total potential energy in the system.
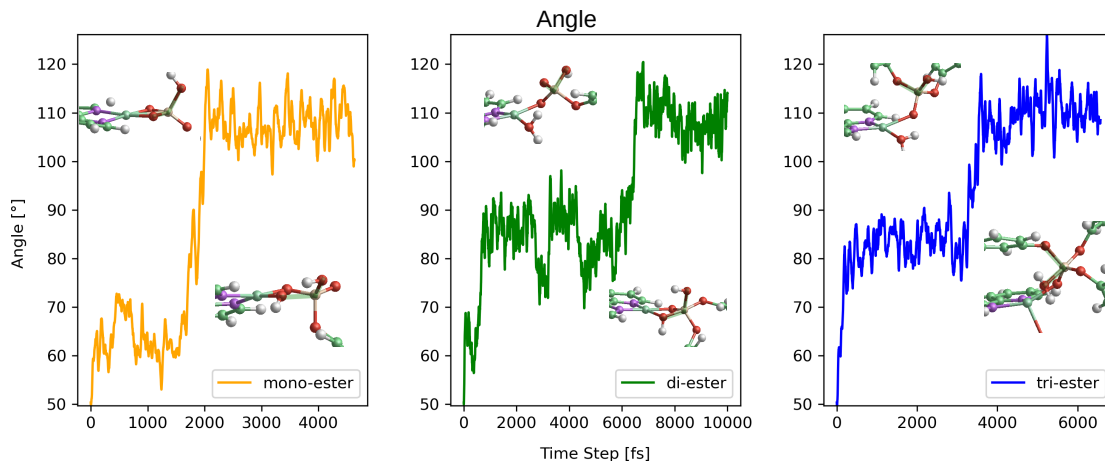
Supplementary Figure 2

Figure 2: Changes in the angle ∠NucO-P-O through the metadynamics. In the mono-ester reactive state (RS), the angle is around 60°. The nucleophile can not form the phosphorane state, in contrast to the di- and tri-ester systems.[2] In di- and tri-ester, the RS is characterized by a ∠NucO-P-O of 90°, indicating the formation of the phosphorus pentavalent state. For all the systems, the product state exhibits an angle of ∼ 110°, which indicates a similar tetrahedral conformation for the phosphates.
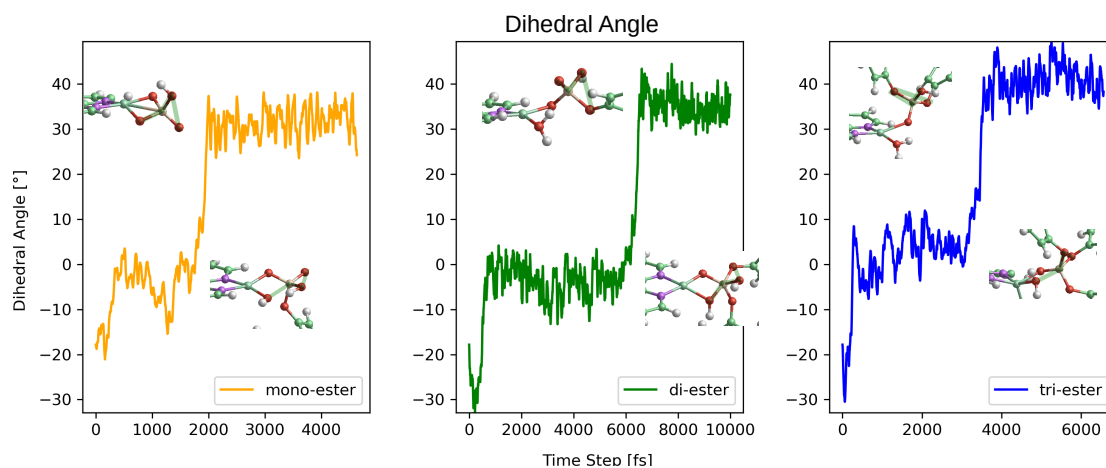
Supplementary Figure 3

Figure 3: Changes in the angle NucO-P-O_1-O_2 through the metadynamics. The reaction can also be characterized through changes in the dihedral angle NucO-P-O_1-O_2, highlighted in the structures. The three kind of phosphates reach the RS stabilization when NucO-P-O_1-O_2 angle is around 0°. For product states (PS), the dihedral angle shows an increase from mono- to di- and tri-ester, taking into account the steric hindrance and the substitution degree.[3,4]
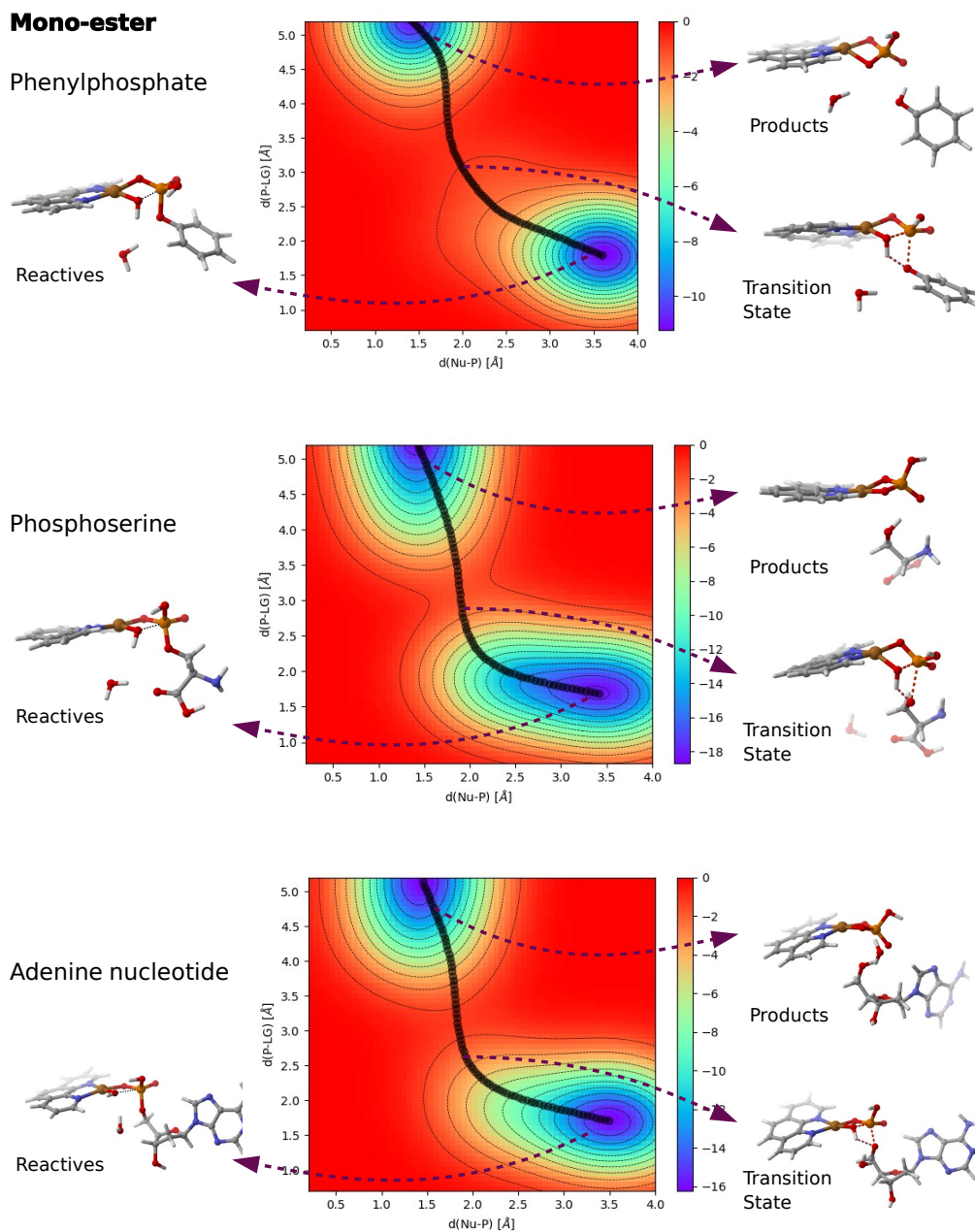
Supplementary Figure 4

Figure 4: Free Energy Surfaces (FES) for all the mono-ester analyzed in this work. The approximate positions of RS, PS and Transition States (TS) are shown. The depicted structures[5] for RS and PS exhibit the most representative conformation in the trajectory. Also, the calculated minimum energy pathway[6,7] for each surface is presented. Energy units for free energy are [kcal/mol].

Supplementary Figure 5

Di-ester

Diphenylphosphate

Dietylphosphate

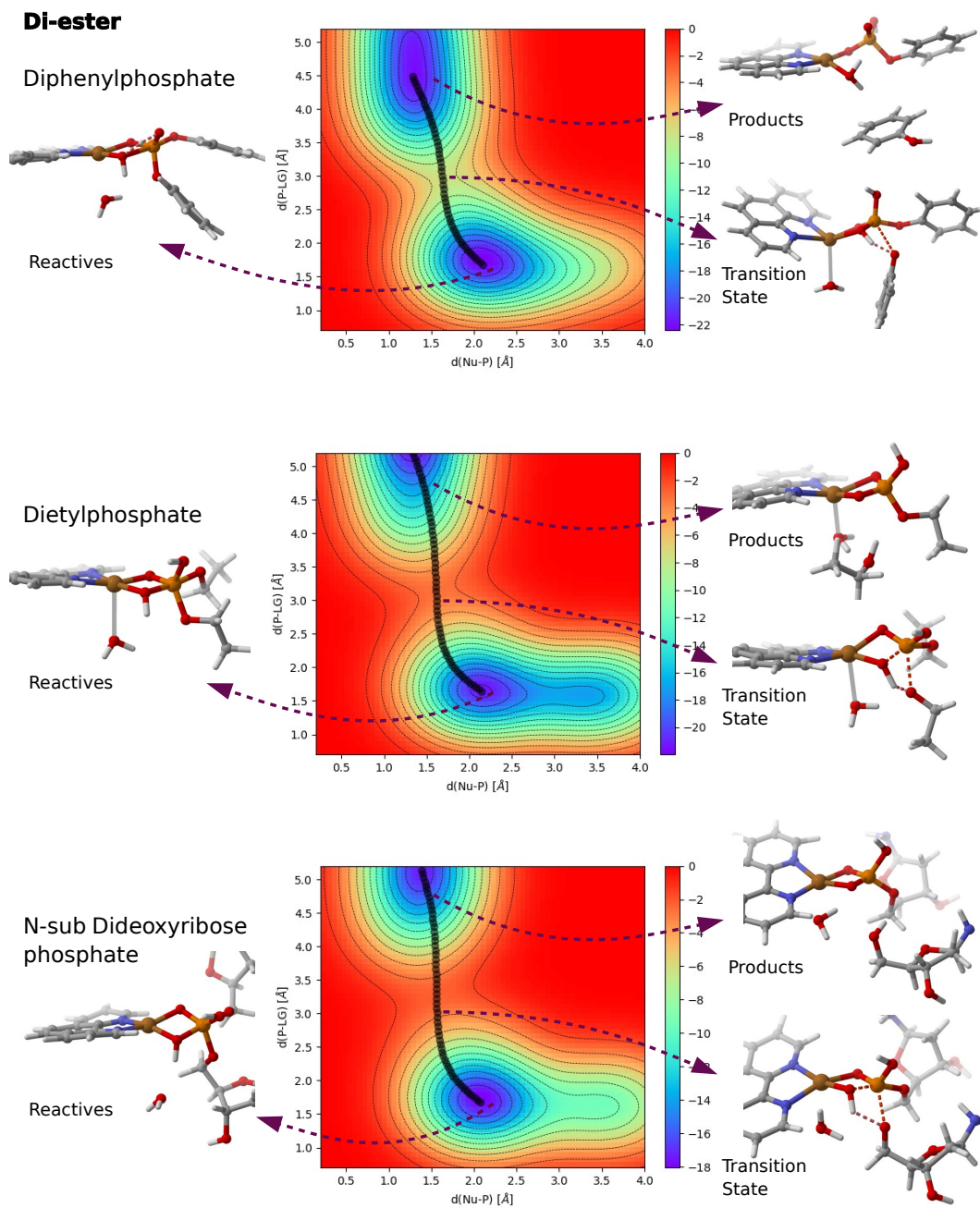N-sub Dideoxyribose phosphate

Figure 5: Free Energy Surfaces (FES) for all the di-ester analyzed in this work. The approximate positions of RS, PS and Transition States (TS) are depicted. The structures for RS and PS exhibit the most representative conformation in the trajectory. Energy units [kcal/mol]

Supplementary Figure 6

Tri-ester

Triphenylphosphate

Reactives

Products

Transition State

Ethyl Diphenilphosphate

Reactives

Products

Transition State

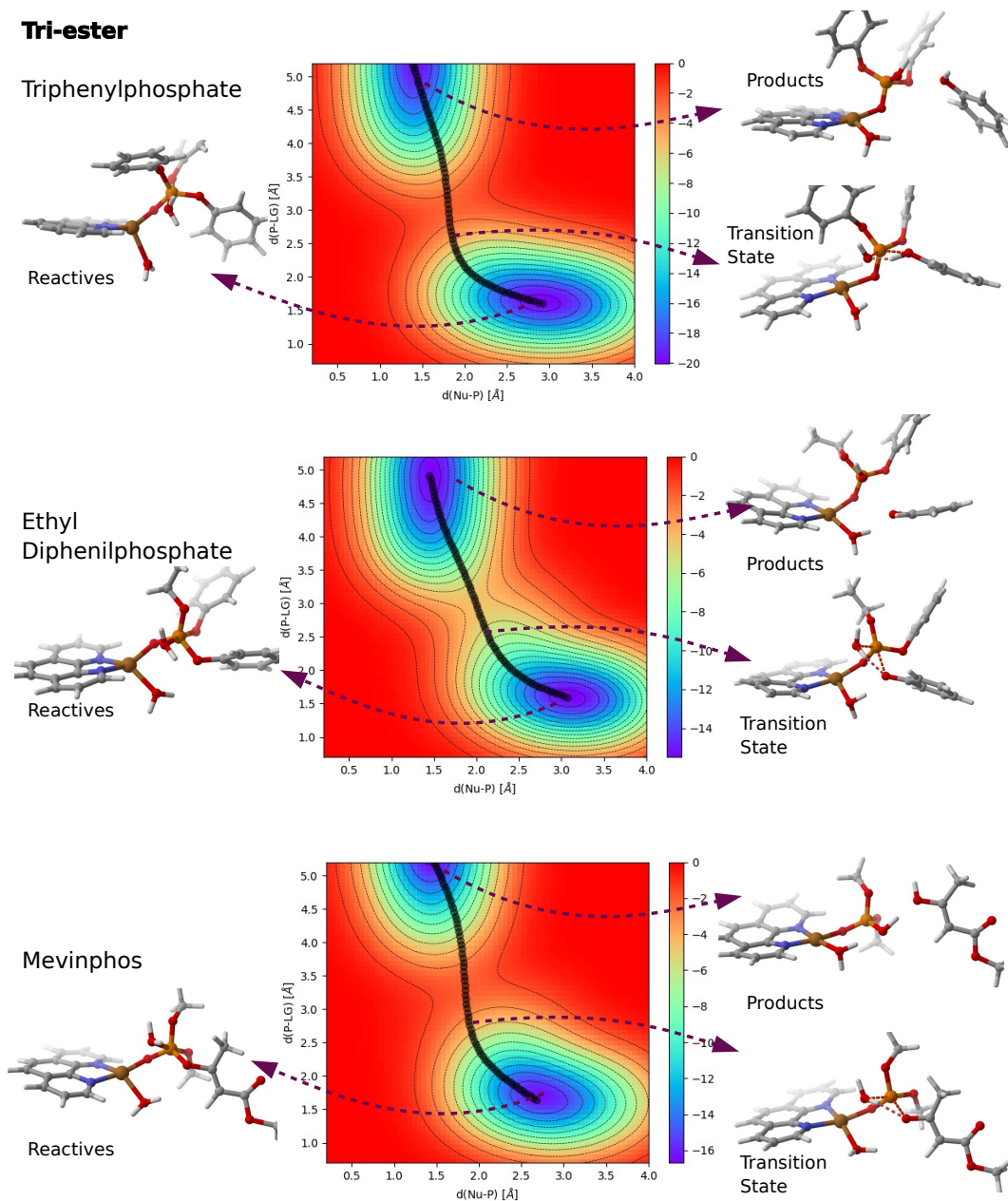Mevinphos

Reactives

Products

Transition State

Figure 6: Free Energy Surfaces (FES) for all the tri-ester analyzed in this work. The approximate positions of RS, PS and Transition States (TS) are depicted. The structures for RS and PS exhibit the most representative conformation in the trajectory. Energy units [kcal/mol]

Supplementary material 7

For each system, a .mp4 movie is presented inside the *movies-reaction.zip* file. The animation shows the precise moment where the nucleophile attacks the P center and then the leaving group abandons the substrate. The simulations are visualized in VMD[8] and exported employing Kazam.[9]
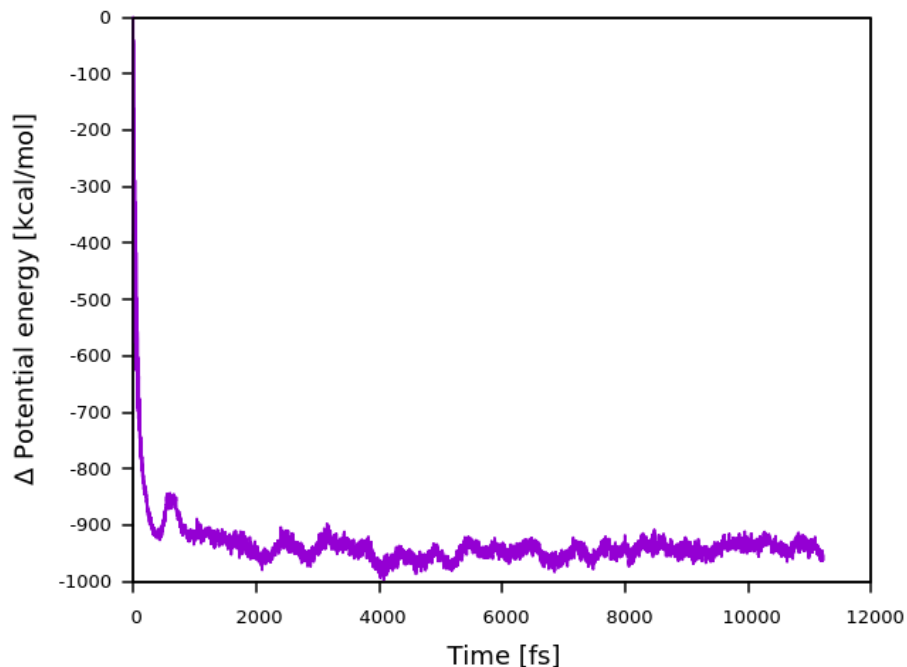
Supplementary material 8

Figure 7: ΔPotential energy graph as a function of time for the equilibration process of $[\mathrm{Cu}^{(\mathrm{II})}(1,10\text{-phenanthroline})(\mathrm{H}_2\mathrm{O})_{54}(\mathrm{PO}_4)]^-$ system.

Figure 8: Temperature graph as a function of time for the equilibration process of $[\text{Cu}^{(\text{II})}(1,10\text{-}$ phenanthroline$)(\text{H}_2\text{O})_{54}(\text{PO}_4)]^-$ system.

Figure 9: Pressure graph as a function of time for the equilibration process of $[\text{Cu}^{(\text{II})}(1,10\text{-}$ phenanthroline$)(\text{H}_2\text{O})_{54}(\text{PO}_4)]^-$ system.
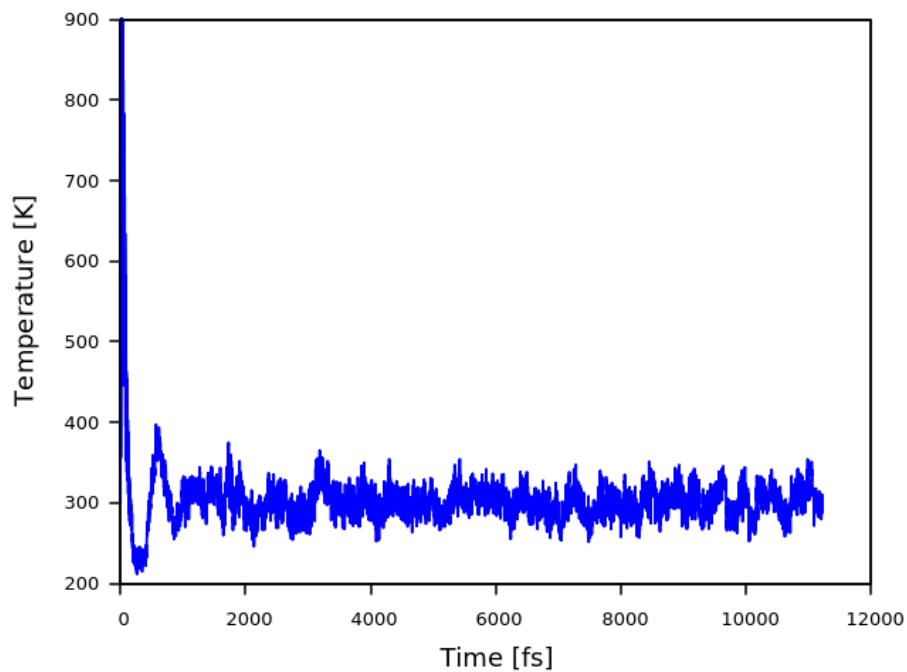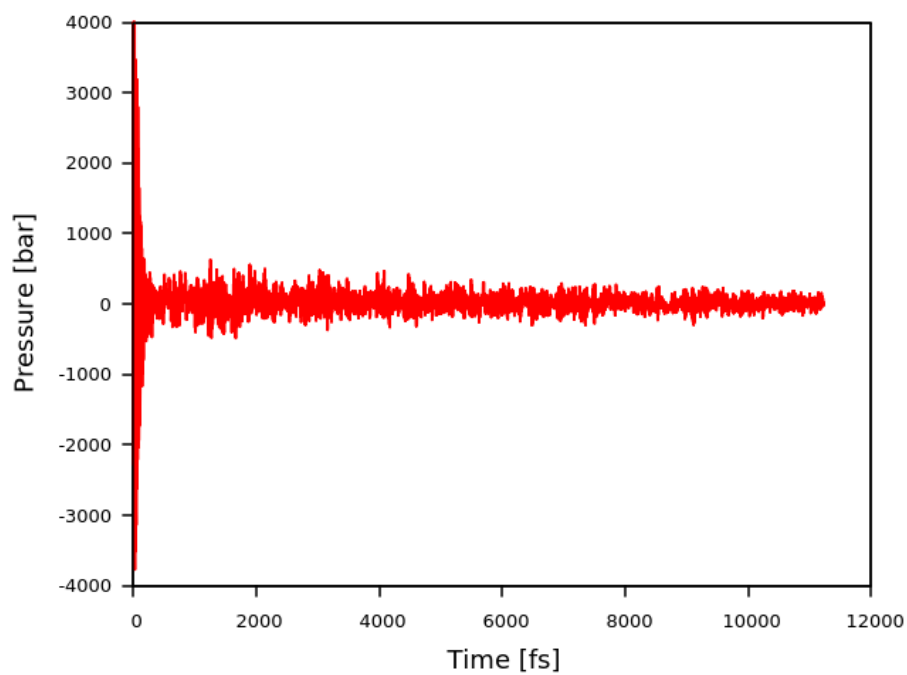
Supplementary material 9

Table 1: Average trajectory time for Well-Tempered Metadynamics (WTMTD) simulations.

Monoester	WTMTD trajectory time (ps)
Phenylphosphate	3.4
Phosphoserine	6.7
Adenine nucleotide	5.6
Diester	
Diphenylphosphate	13.0
Diphenylphosphate	17.8
N-substituted dideoxyribosephosphate	6.0
Triester	
Triphenylphosphate	9.7
Ethyl diphenilphosphate	10.1
Mevinphos	10.0

References

(1) Hutter, J.; Iannuzzi, M.; F,; Schiffmann,; Vandevondele, J. Cp2k: Atomistic simulations of condensed matter systems. Wiley Interdisciplinary Reviews: Computational Molecular Science **2014**, 4, 15–25.

(2) Jonathan K. Lassila, a. D. H., Jesse G. Zalatan Biological phosphoryl-transfer reactions: Understanding mechanism and catalysis. Annual Review of Biochemistry **2011**, 80, 669–702.

(3) Duarte, F.; Barrozo, A.; Åqvist, J.; Williams, N. H.; Kamerlin, S. C. The Competing Mechanisms of Phosphate Monoester Dianion Hydrolysis. Journal of the American Chemical Society **2016**, 138, 10664–10673.

(4) Gallegos, M.; Costales, A.; Ángel Martín Pendás, A real space picture of the role of steric effects in <scp> S _N 2 </scp> reactions. Journal of Computational Chemistry **2022**,

(5) Claude Y. Legault, CYLview20. Université de Sherbrooke, 2020.

(6) Marcos-Alcalde, I.; Setoain, J.; Mendieta-Moreno, J. I.; Mendieta, J.; Gomez-Puertas, P. MEPSA: Minimum energy pathway analysis for energy landscapes. Bioinformatics **2015**, 31, 3853–3855.

(7) Dijkstra, E. W. A Note on Two Problems in Connexion with Graphs. 1959.

(8) Humphrey, W.; Dalke, A.; Schulten, K. VMD – Visual Molecular Dynamics. Journal of Molecular Graphics **1996**, 14, 33–38.

(9) Kazam Team, Kazam. `https://launchpad.net/kazam`.